The t expansion and SU(3) lattice gauge theory

C. P. van den Doel and D. Horn
School of Physics and Astronomy, Tel-Aviv University, Tel-Aviv, Israel
(Received 24 July 1985; revised manuscript received 17 December 1985)

This paper presents the first results obtained by applying the t expansion to the case of an SU(3) lattice gauge theory in $3+1$ space-time dimensions. We apply to this problem the same techniques which have been successfully used in the analysis of the SU(2) theory. We test their effectiveness first on the one-plaquette SU(3) problem, and conclude that even a moderate series in t suffices to reach the weak-coupling domain. We then compute the t expansion of the vacuum energy density to order t^8 and find from our analysis the behavior of this quantity as a function of the coupling constant. From the same series we obtain the mass M of the lowest-lying 0^{++} glueball to order t^6. Evaluating the string tension σ to the same order we construct the ratio $R=M^2/\sigma$ which allows us to obtain a dimensional result for M which is consistent with Monte Carlo analyses.

I. INTRODUCTION

We present calculations of the ground-state energy density $\mathscr{E}$, the string tension σ, and the mass of the lowest-lying 0^{++} glueball M, for the case of a pure SU(3) gauge theory in $3+1$ dimensions. These calculations make use of the t expansion, a nonperturbative calculational tool that was introduced in Ref. 1 and applied to the SU(2) lattice gauge theory in Ref. 2.

In Sec. II we recapitulate the basic elements of the t-expansion technique and the methods that have been developed for its analysis. We test these methods on the one-plaquette problem in Sec. III. We learn from this exercise on a solvable SU(3) problem that a t expansion to order 7 or 8 suffices to reconstruct the energy over the whole strong-coupling domain and well into the weak-coupling regime. Since the series for the mass gap is shorter by two powers of t, its reconstruction in the weak-coupling regime suffers from a large margin of error. Nonetheless the average of diagonal Padé approximants reproduces well the exact result.

The one-plaquette matrix elements are used as an input into the calculation of the energy density in the $(3+1)$-dimensional problem analyzed in Sec. IV. Evaluating the series to order t^8 we have to add connected matrix elements that involve up to three neighboring plaquettes as well as the six plaquettes that close on a cube. For the calculation we use a diagrammatic technique which we briefly outline in the Appendix. After obtaining the energy density we turn to a calculation of the mass gap M and the string tension σ. Both are calculated to order t^6. By analyzing the ratio M^2/σ we obtain a dimensional value for the mass in the weak-coupling domain which is consistent with Monte Carlo results.

II. THE t EXPANSION FOR SU(3) IN THE STRONG-COUPLING BASIS

The theory we study is the $(3+1)$-dimensional SU(3) lattice gauge theory defined by the Kogut-Susskind Hamiltonian[3]

$$H=\frac{g^2}{2}\left[\sum_l \mathbf{E}_l{}^2+x\sum_p(6-\mathrm{tr}U_p-\mathrm{tr}U_p^\dagger)\right], \tag{2.1}$$

where g is the coupling constant and $x\equiv 2/g^4$. The link operators $\mathbf{E}_l$ and U_l which appear in (2.1) are conjugate quantum variables satisfying the commutation relations

$$[E_l^a,U_{l'}]=\frac{\lambda^a}{2}U_l\delta_{ll'}\ . \tag{2.2}$$

Intuitively, the operator E_l^a is the color electric flux operator associated with the link l, and $\mathrm{tr}U_p$ is the color magnetic flux operator associated with the plaquette p. The operator U_p is defined to be

$$U_p=U_1U_2U_3{}^{-1}U_4{}^{-1}\ , \tag{2.3}$$

where the product of the unitary link operators U_l is taken in the counterclockwise direction. In carrying out explicit computations it is useful to work with the operator

$$\overline{H}=\sum_l \mathbf{E}_l{}^2-x\sum_p(\mathrm{tr}U_p+\mathrm{tr}U_p^\dagger)\ , \tag{2.4}$$

which is related to (2.1) by an overall multiplicative and additive constant.

In our analysis we employ the t expansion in the same way in which it was applied to the SU(2) theory in Ref. 2. Using the vacuum of the strong-coupling limit $|0\rangle$, which is the state annihilated by the color-electric field

$$\mathbf{E}_l\,|\,0\rangle=0\ , \tag{2.5}$$

we define the energy function

$$E(t,g^2)=\frac{\langle 0\,|\,He^{-t\overline{H}}\,|\,0\rangle}{\langle 0\,|\,e^{-t\overline{H}}\,|\,0\rangle}\ . \tag{2.6}$$

This function tends in the limit $t\to\infty$ to the correct vacuum energy. The Taylor series of this function defines the connected matrix elements:

$$E(t)=\frac{g^2}{2}\sum_{n=0}^{\infty}\frac{(-t)^n}{n!}\langle\overline{H}^{n+1}\rangle^c+\frac{6V}{g^2}\ . \tag{2.7}$$

Here V is the total volume (number of plaquettes) of the system. E is an extensive quantity and so are all the connected matrix elements. It was shown in Ref. 1 that the connected matrix elements for any Hamiltonian H and trial wave function $|\psi_0\rangle$ obey the recursion relations

$$\langle H^{n+1}\rangle^c = \langle\psi_0|H^{n+1}|\psi_0\rangle - \sum_{p=0}^{n-1}\binom{n}{p}\langle H^{p+1}\rangle^c\langle\psi_0|H^{n-p}|\psi_0\rangle\ , \tag{2.8}$$

which can be used for their algebraic evaluation.

From the energy function one can extract both the vacuum energy and the glueball mass (first excitation). The latter is given by the $t\to\infty$ limit of the expression[2]

$$M(t)\equiv -\frac{g^2}{2}\frac{\partial}{\partial t}\ln\left[-\frac{\partial E(t)}{\partial t}\right]\ . \tag{2.9}$$

The third quantity that we calculate is the string tension. This is obtained by calculating the difference between the ground-state energies of the sector with a string of length L and the sector without any string. The tension $\sigma(t,g^2)$ is defined by dividing this difference by the length L of the string and taking the limit $L\to\infty$. Thus to calculate $\sigma(t,g^2)$ we compute

$$\sigma(t,g^2)=\lim_{L\to\infty}\frac{1}{L}\left[\frac{\langle 0|S^\dagger He^{-t\bar{H}}S|0\rangle}{\langle 0|S^\dagger e^{-t\bar{H}}S|0\rangle}-E(t,g^2)\right]\ , \tag{2.10}$$

where the operator S creates a straight infinite string along one axis; i.e.,

$$S=\prod_{l=(-L/2,0,0)}^{(L/2,0,0)}U_l\ . \tag{2.11}$$

All these quantities refer, of course, to values of operators defined for lattice QCD. To extract physical information we have to study quantities which are expected to scale in the continuum limit. Such a quantity is the ratio

$$R\equiv\frac{M(t)^2}{\sigma(t)}\ . \tag{2.12}$$

Having obtained an algebraic series for both $\sigma(t)$ and $M(t)$ we are in a position to construct one also for R. This was used in Ref. 2 to compare t-expansion results with Monte Carlo calculations. We expect this approach to enable us eventually to calculate the hadron spectrum by algebraic methods.

III. THE ONE-PLAQUETTE PROBLEM

All the connected matrix elements which correspond to diagrams in which the magnetic term $x(\mathrm{tr}U_p+\mathrm{tr}U_p^\dagger)$ hits one and the same plaquette p can be simply evaluated by considering the one-plaquette Hamiltonian

$$H_{\mathrm{op}}=\frac{g^2}{2}\bar{H}_{\mathrm{op}}+\frac{6}{g^2}\ , \tag{3.1}$$

$$\bar{H}_{\mathrm{op}}=4C-x[\chi(3)+\chi(\bar{3})]\ , \tag{3.2}$$

where $\chi(3)$ is the character of the 3 representation and C is the quadratic Casimir operator of SU(3). These matrix elements play a dominant role in the first few terms of the t expansion. In this section we will evaluate them and perform an analysis of the resulting series by the means developed in Ref. 2. The results will then be compared with the values obtained from the diagonalization of this Hamiltonian on a finite Hilbert space. This way we can check our methods of analysis on a solvable SU(3) problem. This will also give us an opportunity to establish the approximate location of the crossover region from strong to weak coupling and to see if the order to which we carry out the t expansion is sufficient to reach into the weak-coupling regime.

The calculation of the connected matrix elements proceeds in a straightforward manner, by first calculating moments of $\bar{H}_{\mathrm{op}}$ using standard SU(3) properties, and then inserting them into (2.8). Thus we find the t expansion:

$$E_{\mathrm{op}}(t,g^2)=\frac{6}{g^2}+\frac{g^2}{2}\left[-t(2x^2)+\frac{t^2}{2!}\frac{2}{3}x^2(-3x+16)-\frac{t^3}{3!}\frac{64}{9}x^2(-3x+8)+\frac{t^4}{4!}\frac{2}{27}x^2(135x^3-2304x+4096)+\cdots\right]\ . \tag{3.3}$$

We replace the variables g^2 and x by a new variable $y=2/g^2$. The energy takes then the form of a double series:

$$E_{\mathrm{op}}(t,y)=3y-\frac{t}{2}y^3+\frac{t^2}{24}y^3(-3y^2+32)+\frac{4t^3}{27}y^3(3y^2-16)+\frac{t^4}{10\,368}y^3(135y^6-9216y^2+32\,768)+\cdots\ . \tag{3.4}$$

We have calculated all terms of this series up to t^8. In so doing we had to evaluate the operation of H_{op} on nine different SU(3) characters, corresponding to the representations **1,3,6,8,10,27,15,15′,24** and their complex conjugates.

For the calculation of the one-plaquette problem we can employ a better method than the t expansion, i.e., diagonalize the Hamiltonian. Figure 1 shows the results of the diagonalization of H_{op} on a nine-dimensional Hilbert space spanned by states corresponding to the SU(3) characters mentioned above. To make sure that these results describe correctly the features of the one-plaquette problem and do not suffer from the truncation of the Hilbert space, we repeated this exercise with a 12-dimensional

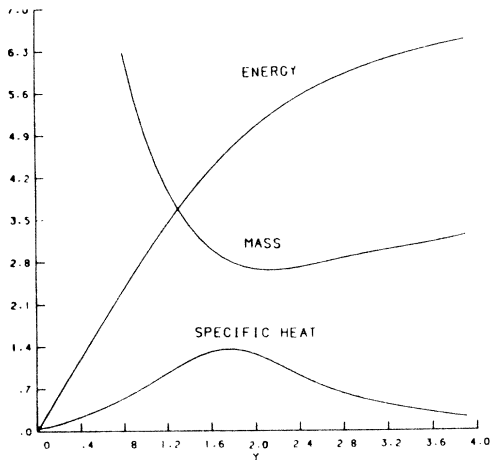

FIG. 1. Results of the diagonalization of the one-plaquette Hamiltonian.

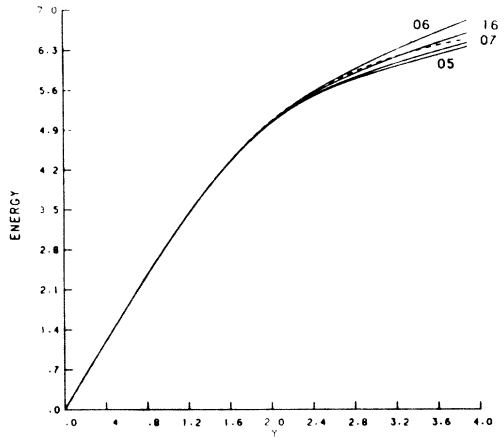

FIG. 2. Comparison of four different D-Padé approximants of the one-plaquette energy with the correct result (dashed curve). Numbers represent the values of L and M (powers of the numerator and denominator) of the corresponding D-Padé approximants. The abscissa is $y=2/g^2$.

Hilbert space into which we added states corresponding to the representations **21,35,42** and their complex conjugates. All results remained stable over the range of $0<y<4$ depicted in Fig. 1. These results include the ground-state energy $E_{\rm op}$, the mass gap (i.e., the difference between the two lowest eigenvalues of $H_{\rm op}$) and the specific heat defined by

$$C=-\frac{d^2E}{dy^2}\ . \tag{3.5}$$

The latter peaks around $y=1.8$. This may then be naturally interpreted as the transition point between the strong-coupling region (low $y=2/g^2$) and the weak-coupling region (high y). It is important to realize that the truncated Hilbert space that we have used was sufficient to cover this transition region. Our aim in the calculation of the $(3+1)$-dimensional problem is to obtain a faithful description of the physics beyond the transition point. If the t expansion of (3.4) can reproduce the features of these curves past this point, we have some chance of extracting physical results from a t expansion to a similar order of the vacuum energy density in $3+1$ dimensions.

We use the D-Padé method[1,2] to analyze the t expansion of the vacuum energy. To form an (L/M) D-Padé approximant of E one integrates from $t=0$ to $t=\infty$ an ordinary (L/M) Padé approximant of dE/dt. L and M are the respective powers of the polynomials in t which appear in the numerator and denominator of the Padé approximant to dE/dt. They are constrained by the conditions

$$M\geq L+2,\quad L+M\leq N-1\ . \tag{3.6}$$

N is the degree of the polynomial which we use for the t series of E.

Once the D-Padé procedure is carried out we are left with some function of y which we can compare with the results of the diagonalization. Such a comparison is carried out in Fig. 2. Here we plot several D-Padé approximants to $E_{\rm op}$ and compare them with the correct answer. All agree very well with the energy in the strong-coupling region and start to deviate from it after passing into the weak-coupling domain. Yet, even there, they outline correctly the range where the energy lies. Figure 3 draws a similar comparison between the second y derivatives of these curves: all display the same behavior in the crossover region.

The (L/M) D-Padé approximants displayed in these two figures are the ones corresponding to the highest values of $L+M$ which are also consistent with one another. The approximants (1/5) and (2/4) have some singular behavior at low y values and were therefore excluded. All the approximants show a tendency to increase faster than the correct curve in the weak-coupling region. This problem was solved in Ref. 2 by using a D-Padé analysis of dE/dy which is then integrated over y to serve as an approximant for E. Moreover, since dE/dy has to be nonnegative, this procedure has a natural cutoff, i.e., the point where the approximant to dE/dy vanishes. Using this procedure we obtain Fig. 4. The new approximants do

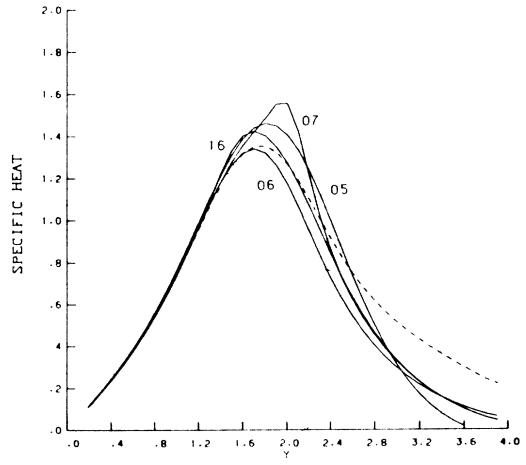

FIG. 3. Specific-heat curves for the same approximants that are displayed in Fig. 2. Notation is identical.

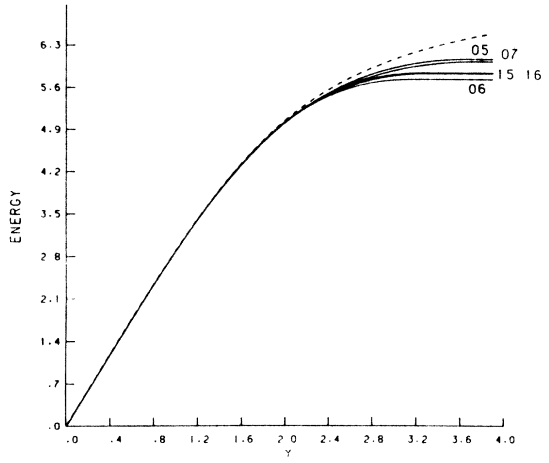

FIG. 4. Comparison of several integrated D-Padé approximants to dE/dy. When the approximant to dE/dy turns negative this function is assumed to remain zero and its resulting curve for E becomes flat. The approximants based on the t series of order 6 or 7 fall short of the correct values in the weak-coupling region of the one-plaquette problem although they are successful in the problem in $3+1$ dimensions.

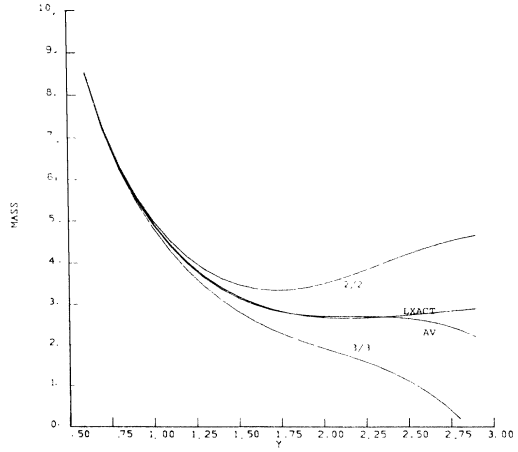

FIG. 5. Comparison of diagonal Padé approximants (evaluated at $t=1000$) to the mass gap of the one-plaquette problem. The curve denoted AV is the average of the (2/2) and (3/3) approximants.

not increase any more like the ones in Fig. 2. In fact they fall below the exact curve. Hence, the dE/dy procedure is not very successful in the one-plaquette problem. It should be noted that the one-plaquette problem is different in this respect from the $(3+1)$-dimensional problem. The latter has a tendency to a much sharper crossover between the strong- and the weak-coupling regions. This can be seen, e.g., in Fig. 1 of Ref. 4 which shows a comparison between the energy curves for these two cases in the SU(2) theory. In our analysis of the $(3+1)$-dimensional problem we will therefore prefer the dE/dy procedure after all. We will see that it leads to results which lie appropriately below an upper limit for the energy density that can be derived at $g=0$, whereas the direct D-Padé approximants to E violate this limit beyond the crossover region.

Finally let us test the t-expansion analysis of the mass. Since we expanded the vacuum energy to order t^8 we can obtain from (2.9) a t expansion for the mass to order t^6. In trying to reconstruct the exact result from the t series, we found that the diagonal Padé approximants, evaluated at asymptotic t, gave better results than the D-Padé procedure. In Fig. 5 we compare the (2/2) and (3/3) approximants, together with their average, to the exact result for the mass. We see that although deviations occur near the crossover region, the average of the Padé approximants lies close to the correct curve for quite some range of y, well into the weak-coupling region.

IV. THE SU(3) THEORY ON A CUBIC LATTICE

We are now ready to apply the tools described in the previous sections to the SU(3) theory defined on a cubic lattice in $3+1$ dimensions. We can make use of all the connected matrix elements calculated for the one-plaquette problem. They represent the repetitive action of the Hamiltonian on a single plaquette. To these we have to add the connected matrix elements that rise from the repetitive action of the Hamiltonian on neighboring plaquettes. All such diagrams that appear up to order x^6 are depicted in Fig. 6. These diagrams represent only the magnetic part of the Hamiltonian. Every box represents $\mathrm{tr}(U_p+U_p^\dagger)$ and the number denotes how many times the same operator hits the same plaquette. In addition to these magnetic terms one has to take into account the electric terms (i.e., Casimir operators). By applying the electric part to the various links one can obtain contributions to all powers of t. Although the lowest possible power of t for any diagram of order x^n is $n-1$, we find, in general, that the first nonvanishing contribution to the connected matrix element occurs for $n+1$ or more; i.e., at least two operations of the electric term are needed. An exception to the rule is the cube diagram, for which the connected matrix element coincides with the vacuum expectation value. In the Appendix we outline a diagrammatic method of calculation which takes into account the effect of the electric terms and allows us to set up an algorithm for calculating the matrix elements for each diagram.

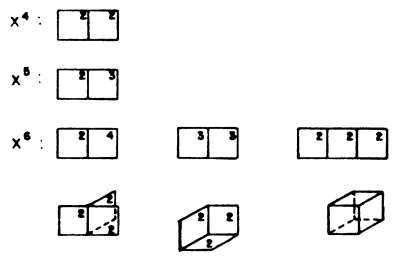

FIG. 6. Diagrams needed for the t expansion. Each square represents the operation of $\mathrm{tr}\,U_p+\mathrm{tr}\,U_p^\dagger$ on a plaquette, and the number shows how many times the same operator was applied to that plaquette. The figure contains all diagrams which involve more than one plaquette at the given order of x.

The quantity that we calculate first is the vacuum energy density $\mathscr{E}$. This is defined as the energy per plaquette, so that the first few powers of t coincide with (3.3). The two expressions start to deviate from one another at order t^5 due to both the x^4 diagram and the cube diagram of Fig. 6. We have carried out the calculation to order t^8 (i.e., H^9). To obtain $\mathscr{E}(y)$ we can use (L/M) D-Padé approximants up to $L+M=7$. Since we deal with a problem in $3+1$ dimensions we use the procedure[2] of applying the D-Padé method to $d\mathscr{E}/dy$ and integrating the results in y to obtain the curves for $\mathscr{E}$ which are presented in Fig. 7. The integration is stopped at the point where an approximant turns negative, since $d\mathscr{E}/dy$ should be a positive-definite quantity. Hence the point at which a curve of $\mathscr{E}$ turns constant is where the approximant failed the positivity condition. The curves plotted in Fig. 7 were those for which this range was the largest. They are consistent with one another for quite some range inside the weak-coupling domain.

In the weak-coupling limit the SU(3) problem turns into a gauge theory of eight independent gauge fields on each link. Using the harmonic approximation one can obtain therefore the value of $\mathscr{E}(y\to\infty)=6.368$. This number should serve as an upper limit on $\mathscr{E}(y)$. Figure 7 is consistent with it.

The specific-heat curves for the same three approximants that are plotted in Fig. 7 are shown in Fig. 8. All curves peak between $y=1.5$ and 1.7. This should therefore be identified with the crossover region between strong and weak coupling.

Using the t expansion of the vacuum energy to eighth order, we can derive one for the mass out to sixth order in t. This technique was tested for the one-plaquette problem, where we concluded that the average of the approximants gave a fair description of the true mass. Here we are dealing with a physical problem for which we can start to be more ambitious and try to derive a value of the mass in dimensional units. To achieve this we have to calculate first a t expansion for the string tension. Once this is done we form the ratio $R=M^2/\sigma$. This ratio should scale in the weak-coupling limit, and from it we can obtain a prediction for the mass. Since we have an expansion for the mass to sixth order in t, we need a comparable expansion for the string tension. We obtain the following result:

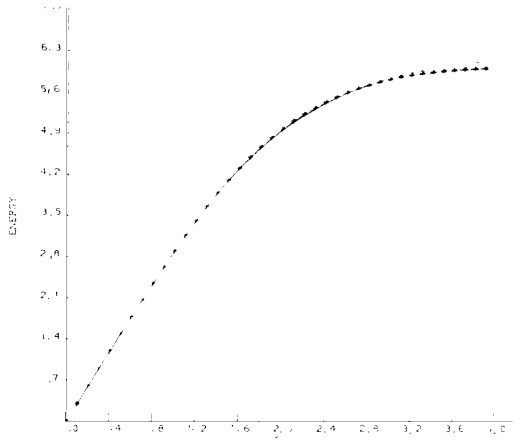

FIG. 7. The energy density as reconstructed from D-Padé approximants to dE/dy. Shown are (0/6), (0/7), and (1/6) approximants, represented by a line, $+$, and $*$, respectively. Results should be compared with an upper limit of 6.368.

$$\sigma(t,g^2)=\frac{g^2}{2}\left[\tfrac{4}{3}+x^2(-32t^3/27+116t^4/27-76t^5/9+25562t^6/2187)\right.$$
$$\left.-x^3(20t^4/27-1172t^5/405+21754t^6/3645)+210x^4t^6/405+70x^5t^6/162\right]. \tag{4.1}$$

To get a feeling for the information contained in this series we compare the results of two diagonal Padé approximants (applied to $\partial\sigma/\partial y$, evaluated at asymptotic t, and integrated in y) to the strong-coupling perturbative expansion to order x^6 presented by Kogut.[5] This is shown in Fig. 9. All curves agree all the way down to $y=1.5$. Near $y=2$ the strong-coupling expansion turns negative. This is another (and independent) indication of the location of the crossover region. Clearly the tension has to remain positive; however, it has to look very different from the curves shown here: it has to vanish strongly in y. The fact that it is difficult to obtain such a behavior was already discussed at length in Ref. 2. Nonetheless, there is still a good chance that the ratio R will lead to a meaningful result.

The ratio R is constructed as a ratio of two t expansions. This is then reordered as a single t expansion whose coefficients are functions of y. Having an expansion to order t^6 we can, in principle, construct two diago-

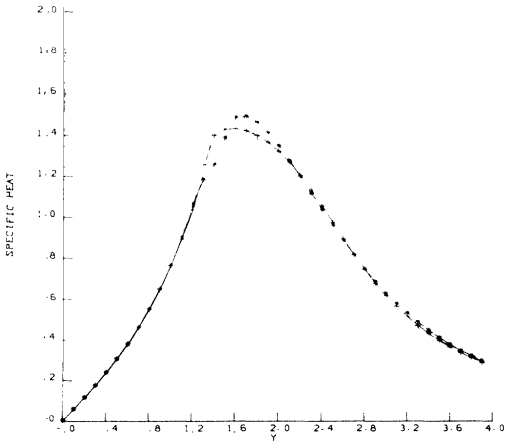

FIG. 8. Specific-heat curves which are obtained by differentiation of the dE/dy approximants whose integrals were displayed in Fig. 7.

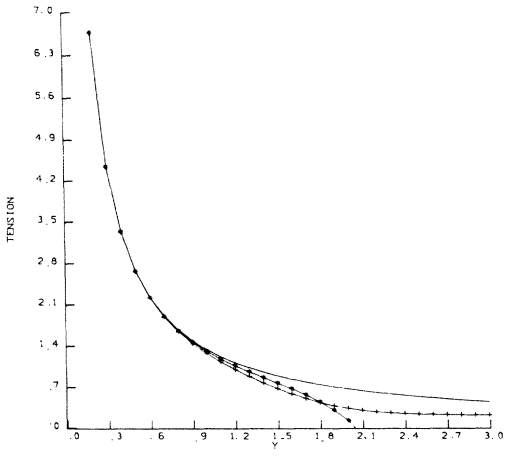

FIG. 9. Comparison of (2/2) and (3/3) Padé approximants for the string tension at asymptotic t with the results of strong-coupling perturbation theory. The three curves are designated by a line, +, and *, respectively. The strong-coupling curve crosses zero in the crossover region.

nal Padé approximants, of orders (2/2) and (3/3). The latter turned out to have a singular y behavior; however, the (2/2) approximant displays a plateau around $R \approx 10$. An even more stable result is obtained by applying the diagonal Padé (evaluated at asymptotic t, e.g., $t=1000$) to dR/dy and then integrating it in y. These two curves are displayed in Fig. 10 together with two other curves that were obtained from D-Padé analyses. The D-Padé procedure was also applied to dR/dy. Shown are the averages of the (0/4) and (1/3)—as well as the average of the (0/5) and (1/4)—D-Padé approximants. Although the separate D-Padé approximants show a wider dispersion,

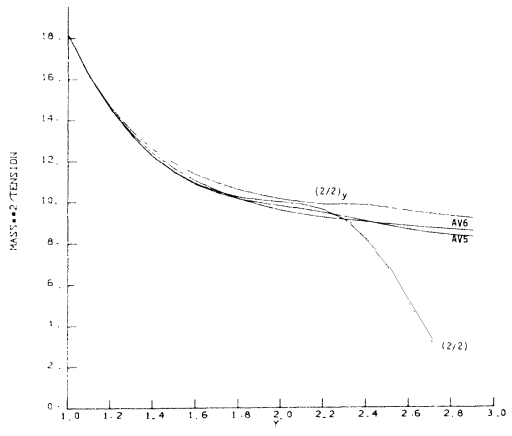

FIG. 10. Four different approximants to $R=M^2/\sigma$ which exhibit scaling behavior. They are (2/2) Padé for R, (2/2) Padé for dR/dy integrated in y [designated (2/2)y], the average of the (0/4) and (1/3) D-Padé (for dR/dy) designated by AV5, and AV6 designating the average of the (0/5) and (1/4) D-Padés. AV5 and AV6 include information of the t expansion to order t^5 and t^6, respectively.

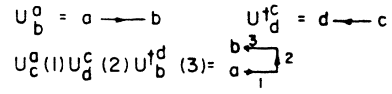

FIG. 11. Diagrammatic notations for the link matrices U.

their averages are very consistent with one another and lie between $9 < R < 10$ in the region around $y \approx 2$.

We expect the curves obtained from the t expansion to develop an envelope that displays a steep descent in the strong-coupling region and settles into a constant in the weak-coupling regime. Interpreting the plateau of Fig. 10 as corresponding to this scaling result we conclude that the mass of the 0^{++} glueball is predicted by this analysis to lie around $3\sqrt{\sigma} \approx 1.3$ GeV. It is encouraging to note that in this first algebraic evaluation of the mass gap in SU(3) we obtain a result which falls within the range of values derived from numerical Monte Carlo analyses (a recent summary of results was presented in Ref. 6).

ACKNOWLEDGMENTS

One of us (D.H.) would like to thank M. Karliner for many helpful discussions and the SLAC theory group for its hospitality during the period in which the manuscript was finalized. This work was supported in part by the U.S.-Israel Binational Science Foundation.

APPENDIX: DIAGRAMMATIC SU(3) CALCULATIONS

In this appendix we outline the method that we use for calculating the matrix elements. We use a diagrammatic language that incorporates the SU(3) properties of the link variables and the topological structure of the cubic lattice. It bears some similarity to the methods that were put forward by Cvitanovic and by Mandula.[7]

Our basic link element is the 3×3 unitary matrix U_b^a

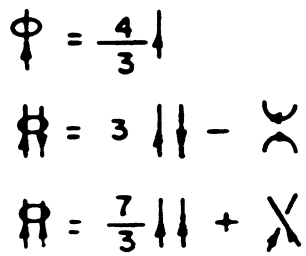

FIG. 12. Application of the Casimir operator (represented by a ring) to link matrices and their products.

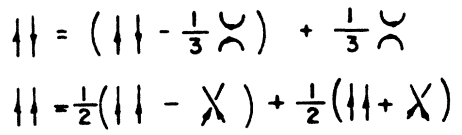

FIG. 13. Decomposition of products into irreducible representations of SU(3).

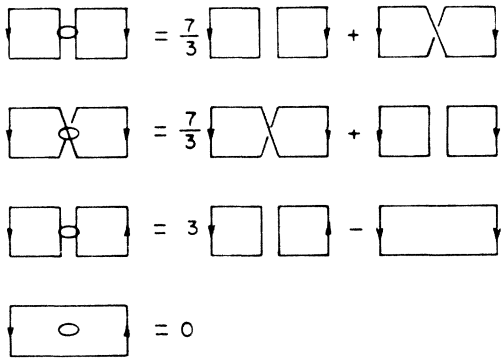

FIG. 14. An algebraic system created by two neighboring plaquette operators ($\mathrm{tr}\,U_p$ or $\mathrm{tr}\,U_p^\dagger$) which is closed under operation by the Casimir of the common link.

which is an element of SU(3). Following Kogut and Susskind[3] we represent it by a vector which lies on the link with which U is associated. This notation is shown in Fig. 11. If the arrow points along a positive direction it represents U, and if it points in a negative direction it represents $U^\dagger$. Arrows which are attached to one another imply the obvious operation of matrix multiplication as shown in this figure. A closed loop will therefore represent the trace over the corresponding product of matrices. In our calculations we have to evaluate matrix elements of products of such closed loops. These loops are generated by the magnetic term of our Hamiltonian, and are modified by the operation of the electric term, which is the sum over the quadratic Casimir operators of all links.

The link element U_b^a is, in fact, a representation of SU(3)×SU(3). The two different SU(3) groups are associated with the two vertices on the two ends of the link. The notation that one uses in the electric term of the Hamiltonian refers to just one set of these SU(3) generators. By convention it is chosen to operate on the left (or low) end of the link. This is the choice implied by the basic algebraic equation

$$[E^a,U]=\frac{\lambda^a}{2}U\ . \tag{A1}$$

The effect of the Casimir operator is given by the double commutator

$$[E^a[E^a,U]]=\tfrac{4}{3}U\ . \tag{A2}$$

This is represented by a ring around the vector in Fig. 12. The two other equations on this figure show what happens when the double commutator acts on an exterior product of two U matrices associated with the same link. Thus the second diagram shows the effect of acting on $U_b^a U_d^{\dagger c}$. The result is that the same object is returned with a factor of 3, but, together with it one obtains $-\delta_d^a\delta_b^c$.

One can use the results of the Casimir operation to decompose the exterior product into irreducible representations of SU(3). Figure 12 shows cases corresponding to the direct products of 3×3 and $3\times\bar{3}$. Using the known eigenvalues of the Casimir operator one obtains the decomposition shown in Fig. 13 which corresponds to

$$3\times\bar{3}=8+1,\quad 3\times3=\bar{3}+6\ .$$

There are several ways to proceed with the calculation. One may start by decomposing a given set of products of loops into a set of orthonormal states which behave as irreducible representations under SU(3) rotations of every link. Once this decomposition is given, one can either calculate every order of the electric term separately, or calculate all orders at once by using the perturbative approach (Sec. V in Ref. 1). The latter is also particularly useful to obtain the strong-coupling perturbation-theory result from the same calculation.

We found it easier to use an alternative approach. Starting with a given set of products of loops we note that by applying the electric term one obtains the same diagrams as well as new ones. After several applications of these Casimir operators this set of diagrams closes. An example is shown in Fig. 14. Here we insert the results of Fig. 12 between two neighboring plaquettes. These diagrams, as well as their complex conjugates, are all the ones one needs for calculating the contributions of order x^4 in Fig. 6. All orders of the electric term are now well defined. By evaluating the norm of—and the overlap between—the different diagrams, one obtains the necessary input to the calculation. This is the method we have used for diagrams of order x^5 and higher. Once the algebra for a given set of diagrams was defined, we have manipulated it by using the REDUCE computer language to compute all the orders in t that we needed.

[1]D. Horn and M. Weinstein, Phys. Rev. D **30**, 1256 (1984).
[2]D. Horn, M. Karliner, and M. Weinstein, Phys. Rev. D **31**, 2589 (1985).
[3]J. Kogut and L. Susskind, Phys. Rev. D **11**, 395 (1975).
[4]D. Horn and M. Karliner, Nucl. Phys. **B235**, 135 (1984).
[5]J. B. Kogut, Phys. Rep. **67**, 67 (1980).
[6]B. Berg, Nucl. Phys. **A434**, 151c (1985).
[7]P. Cvitanovic, Phys. Rev. D **14**, 1536 (1976); J. E. Mandula, Southampton Report No. SHEP 80/81-7 (unpublished).